Total Variation Based Image and Structure Enhancement for Electron Tomography

Carlos Bazan

February 2007

Publication Number: CSRCR2007-04

Computational Science & Engineering Faculty and Students Research Articles

Database Powered by the Computational Science Research Center Computing Group

COMPUTATIONAL SCIENCE & ENGINEERING

SAN DIEGO STATE UNIVERSITY

Computational Science Research Center
College of Sciences
5500 Campanile Drive
San Diego, CA 92182-1245
(619) 594-3430

Total Variation Based Image and Structure Enhancement for Electron Tomography

Carlos Bazan

February 16, 2007

Abstract

To date, it is firmly established that mitochondrial function plays an important role in the regulation of apoptosis (programmed cell death). There is also evidence that defects in function may be related to many of the most common diseases of aging, such as Alzheimer dementia, Parkinson's disease, type II diabetes mellitus, stroke, atherosclerotic heart disease and cancer. This belief is founded in the observation that mitochondrial function experiences measurable disturbance and observable morphological changes under these circumstances. Electron tomography has allowed significant advances in the understanding of mitochondrial structures. Despite the recent advances in imaging hardware and specimen fixation techniques, the interpretation and measurement of the structural architecture of mitochondria depend substantially on the availability of good software tools for filtering, segmenting, measuring and classifying the features of interest. It has been argued in the structural biology community that the image processing methodologies in the three-dimensional electron tomography field are not yet sufficiently developed, so as to correctly extract features and understand spatial relationships in mitochondrial structures. The main motivation for the proposed work is the development of mathematically sound and computationally robust algorithms for the reduction of noise and enhancement of structural information in mitochondrial images. Our research efforts will initially focus on the understanding of the sources and mechanisms which introduce noise (image degradation) in electron tomography process. Correct modeling of the degradation, will allow us to design effective, correct, algorithms for the removal of the noise without negatively impacting fine-detail structural information, and will allow for a posteriori reconstruction of more accurate three-dimensional mitochondrion images. Our noise reduction and reconstruction efforts will employ a partial differential equation approach based on the minimization of the total variation norm, which has been utilized very successfully in other areas of computer vision.

1 Specific Aims

The objective of this research, from the standpoint of our contribution to public health, is to develop, implement and integrate modern image processing techniques in order to obtain more accurate mitochondrial structural information from data collected using three-dimensional (3-D) electron tomography (ET). The larger goal is to boost the understanding of the intricate mitochondrial architecture and its relation to functionality. The work is relevant in particular to the structural biology community and to its contribution to public health through the understanding of biological systems.

To date, it is firmly established that mitochondrial function plays an important role in the regulation of apoptosis (programmed cell death) [41]. There is also evidence that defects in function may be related to many of the most common diseases of aging, such as Alzheimer dementia, Parkinson's disease, type II diabetes mellitus, stroke, atherosclerotic heart disease and cancer [78]. This belief is founded in the observation that mitochondrial function experiences measurable disturbance and observable morphological changes under these circumstances [78, 36]. Electron tomography has allowed significant advances in the understanding of mitochondrial structures. This imaging technique currently provides the highest 3-D resolution of the internal arrangement of mitochondria in thick sections. Despite the recent advances in imaging hardware and specimen fixation techniques, the interpretation and measurement of the structural architecture of mitochondria depend substantially on the availability of good software tools for filtering, segmenting, measuring and classifying the features of interest.

It has been argued in the structural biology community [36] that the image processing methodologies in the 3-D ET field are not yet sufficiently developed, so as to correctly extract features and understand spatial relationships in mi-

tochondrial structures. There is a strong need for a set of image processing methodologies that will facilitate efficient reconstruction and analysis of the data obtained via ET. The main motivation for the proposed work is the development of mathematically sound and computationally robust algorithms for the reduction of noise and enhancement of structural information in mitochondrial images. We will establish a multi-disciplinary approach, based on a combination of established expertise in the fields of image processing, mathematics, computational science, and structural biology. Our research efforts will initially focus on the understanding of the sources and mechanisms which introduce noise (image degradation) in ET process. Correct modeling of the degradation, will allow us to design effective, correct, algorithms for the removal of the noise without negatively impacting fine-detail structural information, and will allow for a posteriori reconstruction of more accurate 3-D mitochondrion images. Our noise reduction and reconstruction efforts will employ a partial differential equation (PDE) approach based on the minimization of the total variation norm, which has been utilized very successfully in other areas of computer vision [18, 20, 21, 27, 91, 92, 107, 24, 108].

2 Background and Significance

The basic stages involved in electron tomography are [36]: a) tilt series acquisition, b) views alignment and normalization, c) tomographic computation and volume reconstruction, d) segmentation and measurement, and e) rendering and visualization. Several software applications and computational techniques have been specifically developed for ET. These packages offer comprehensive sets of tools that allow a wide range of structural biology analyses. The most popular general packages are IMOD [54, 66], SPIDER [8, 35, 125], Protomo [120, 122, 104, 121], SerialEM [67], EM3D [46], XMIPP [96], TOM

[72], EMAN/EMAN2 [63, 103], and UCSF tomography [127, 128]. There are also many tools available that permit specialized tasks such as data acquisition [102, 67, 127, 128, 72, 129], signal filtering [74, 15, 64, 70, 106, 97, 30, 32, 121], image segmentation [61, 110, 88], and data visualization [39, 3, 124, 123].

There have been many technical improvements in computational tools (both hardware and software) aimed at furthering the capability of extracting quantitative information from tomograms. The interpretation and measurement of the substructures of mitochondria depend crucially on the employment of algorithms for segmenting and classifying the features of interest, tools for making 3-D measurements, and software for interactively visualizing components of the structure [78]. Among the most critical aspects within electron tomography are the 3-D filtering and two-dimensional (2-D) and 3-D segmentation processes. The former constitutes the main topic of this research. Below we present the state of the art in the two main PDE-based approaches used for the reduction of noise and the enhancement of local structures in 3-D tomograms.

Anisotropic Nonlinear Diffusion. Anisotropic Nonlinear Diffusion is a very powerful image processing technique used for the reduction of noise and enhancement of structural features. It was first introduced in image processing by Perona and Malik [82] as an attempt to overcome the shortcomings of linear diffusion processes, namely the blurring of edges and other localization problems. The model accomplishes this by applying a process that reduces the diffusivity in places having higher likelihood of being edges. This likelihood is measured by a function of the local gradient $\|\nabla u\|$. The model can be written as

$$\partial_t u - \nabla \cdot \left(g\left(\| \nabla u \|^2 \right) \nabla u \right) = 0, \tag{1}$$

on the image domain Ω, with homogenous Neumann boundary conditions $\partial_{\mathbf{n}} u = 0$ on $\partial\Omega$ (no flux across the image boundary), and initial condition $u(0, x) =$

$u_0(x)$ where $u_0 \in C\left(\mathbb{R}^2\right)$. In this model the diffusivity has to be such that $g\left(\|\nabla u\|^2\right) \to 0$ when $\|\nabla u\| \to \infty$ and $g\left(\|\nabla u\|^2\right) \to 1$ when $\|\nabla u\| \to 0$. One of the diffusivity functions proposed by Perona-Malik, is $g\left(\|\nabla u\|^2\right) = \left(1 + \|\nabla u\|^2 \big/ \lambda^2\right)^{-1}$ where $\lambda > 0$ is a free parameter. Despite the practical success of the Perona-Malik model, it presents some serious theoretical problems [118, 73, 51, 47, 83, 17, 38, 10]. It has been argued [38, 10] that the regularizing effect of the discretization is perhaps the key element in the success or failure of the model. Most practical applications work very well provided that the numerical schemes stabilize the process through some implicit regularization. This observation motivated much research towards the introduction of the regularization directly into the PDE to avoid the dependence on the numerical schemes [17, 73]. A variety of spatial, spatio-temporal, and temporal regularization procedures have been proposed over the years [17, 6, 119, 60, 111, 115]. The one that has attracted much attention is the mathematically sound formulation due to Catté, Lions, Morel and Coll [17]. They proposed to replace the diffusivity $g\left(\|\nabla u\|^2\right)$ of the Perona-Malik model by a slight variation, $g\left(\|\nabla u_\sigma\|^2\right)$, with $u_\sigma = G_\sigma * u$, where G_σ is a smooth kernel (Gaussian). This spatial regularization model belongs to a class of well-posed problems (existence and uniqueness were proven in [17]), and its successful implementation is contingent on choosing an appropriate value for the additional regularization parameter, σ.

Frangakis and Hegerl [33] introduced anisotropic nonlinear diffusion in ET. They proposed a diffusivity matrix $\mathbf{D}$ structured as follows:

$$\mathbf{D} = \begin{bmatrix} \mathbf{v}_1 & \mathbf{v}_2 & \mathbf{v}_3 \end{bmatrix} \begin{bmatrix} \lambda_1 & 0 & 0 \\ 0 & \lambda_2 & 0 \\ 0 & 0 & \lambda_3 \end{bmatrix} \begin{bmatrix} \mathbf{v}_1 & \mathbf{v}_2 & \mathbf{v}_3 \end{bmatrix}^{\mathrm{T}}. \tag{2}$$

The vectors $\mathbf{v}_i$ are the eigenvectors of the image's structure tensor $\mathbf{J} = \nabla u \cdot \nabla u^{\mathrm{T}}$

or its convolved version $\mathbf{J}_\sigma = \mathbf{K}_\sigma * \mathbf{J}$, where $\mathbf{K}_\sigma$ is a Gaussian kernel of width σ. The parameters λ_i are functions of the eigenvalues, $\mu_1 \geq \mu_2 \geq \mu_3$, of the structure tensor $\mathbf{J}$ (or $\mathbf{J}_\sigma$). Together, the eigenvalues μ_i and the eigenvectors $\mathbf{v}_i$, characterize the local structural features of the image u within a neighborhood of size $O(\sigma)$. Each parameter λ_i reflects the variance of the gray level in the direction of the corresponding eigenvector $\mathbf{v}_i$, and has to be chosen carefully.

Frangakis *et al* chose the parameters λ_i to create a hybrid model that combines both edge enhancing diffusion (EED) [112] and coherence enhancing diffusion (CED) [114, 113, 117]. EED is based on the directional information of the eigenvectors of the structure tensor $\mathbf{J}$ and its aim is to preserve and enhance edges. CED is based on the directional information of the eigenvectors of the convolved structure tensor $\mathbf{J}_\sigma$ and it is intended for improving flow-like structures and curvilinear continuities. For EED, the parameters λ_i are chosen following the Perona-Malik model [82] with

$$\lambda_1 = \lambda_2 = g(\mu_1), \quad \lambda_3 = 1, \tag{3}$$

while for CED, they are defined according to

$$\lambda_1 = \lambda_2 = \alpha, \quad \lambda_3 = \alpha + (1-\alpha)\exp\left(-C\Big/(\mu_1 - \mu_3)^2\right), \tag{4}$$

with user-defined free parameters α (regularization constant, typically 10^{-3}) and $C > 0$. Structures with $(\mu_1 - \mu_3)^2 > C$ will be regarded as line-like patters and will be enhanced.

To combine the advantages of EDD and CED the approach presented in [33] uses a switch based on comparing an *ad hoc* threshold parameter[1] to the local relation between structure and noise $(\mu_1 - \mu_3)$. EDD is used when the difference

[1]The threshold is computed from the mean value of $(\mu_1 - \mu_3)$ in a subvolume of the image containing only noise.

$(\mu_1 - \mu_3)$ is smaller than the threshold parameter. When it is larger, the model would switch to CED. In a separate communication, Frangakis, Stoschek and Hegerl [34], applied the hybrid model to 2-D and 3-D synthetic data and compared it with conventional methods as well as with wavelet transform filtering. They concluded that the model exhibits an excellent performance at lower frequencies, achieving considerable improvement in the signal-to-noise ratio (SNR), but that due to the low-pass characteristics of the diffusion and the discretization stencil, high frequencies components of the signal are irreversibly degraded. In [33] the authors applied the model to volumetric data as obtained by electron tomography. A considerable SNR improvement was achieved for both of the examples presented. Thus, it greatly facilitated the posterior segmentation and visualization. They again noted that the method acts as a low-pass filter, and that this is an expected, yet unwanted, effect of the theoretical considerations involved.

Fernández and Li [30, 31] proposed a variant to the model in [33] for ET filtering by anisotropic nonlinear diffusion, capable of reducing noise while preserving both planar and curvilinear structures. They provided the model with a background filtering mechanism that highlights the interesting biological structural features and with a new criterion for stopping the iterative process. The CED model presented in (4) diffuses unidirectionally along the direction of minimum change $\mathbf{v}_3$, and efficiently enhances line-like structures (where $\mu_1 \approx \mu_2 \gg \mu_3$). It was argued in [30] that a significant amount of structural features from biological specimens resemble plane-like structures at local scale. Therefore, the authors defined a set of metrics to discern whether the features are plane-like, line-like or isotropic. The metrics defined are:

$$P_1 = \frac{\mu_1 - \mu_2}{\mu_1}, \quad P_2 = \frac{\mu_2 - \mu_3}{\mu_1}, \quad P_3 = \frac{\mu_3}{\mu_1}, \tag{5}$$

which satisfy $0 \leq P_i \leq 1$, $\forall i$ and $P_1 + P_2 + P_3 = 1$. We should note that μ_1, μ_2 and μ_3 are the eigenvalues of the convolved structure tensor $\mathbf{J}_\sigma$. These metrics are such that when $P_1 > P_2$ and $P_1 > P_3$, we have a plane-like structure; when $P_2 > P_1$ and $P_2 > P_3$, we have a line-like structure; and when $P_3 > P_1$ and $P_3 > P_2$, we have an isotropic structure. To achieve planar enhancing diffusion, equation (4) is modified as follows:

$$\begin{aligned} \lambda_1 &= \alpha, \\ \lambda_2 &= \alpha + (1-\alpha)\exp\left(-C_2 \Big/ (\mu_1 - \mu_2)^2\right), \\ \lambda_3 &= \alpha + (1-\alpha)\exp\left(-C_3 \Big/ (\mu_1 - \mu_3)^2\right). \end{aligned} \tag{6}$$

For the case of isotropic structure the model employs what the authors call "background diffusion" based on Gaussian smoothing.

To address the crucial question of when to stop the filtering process the authors proposed two different criteria. In [30], they proposed a stopping criterion based on the evolution of the variance in the subvolume of noise from which the EED/CED threshold's switch was obtained. The devised a ratio, similar to the one proposed in [114], the relative noise variance

$$r_N(t) = \frac{\mathrm{var}\,(u_N^t)}{\mathrm{var}\,(u_N^0)}, \tag{7}$$

where u_N^0 and u_N^t represent the gray values of the subvolume N at time 0 and t, respectively. Since $r_N(t)$ decreases monotonically from 1 to 0, a suitable threshold can be set based on the desired noise reduction factor. However, since this criterion does not consider the entire volume, it can not guarantee that the signal will not be affected by the diffusion. To avoid this, the authors proposed a different criterion [31] similar to the one proposed in [71]. The noise-estimate variance criterion states that the optimal stopping time is the time (iteration)

in which var $\left(u^0 - u^t\right)$ reaches var $\left(u_N^0\right)$, which can be expressed analytically as

$$t_{\text{stop}} = \arg\min_t \left\{ \left| \text{var}\left(u_N^0\right) - \text{var}\left(u^0 - u^t\right) \right| \right\}, \tag{8}$$

where u^t and u^0 represent the gray values of the whole volume at time 0 and t, respectively.

Total Variation Based Methods. Rudin, Osher and Fatemi [89] proposed image noise removal by minimizing the total variation (TV) norm of the estimated solution. They derived a constrained minimization algorithm as a time-dependent nonlinear PDE, where the constraints are determined by the noise statistics. They stated that the space of bounded total variation is the proper class for many basic image processing tasks. Thus, the restored image is the solution of

$$\min_u \int_\Omega \| \nabla u \| \, dx, \tag{9}$$

subject to the following constraint involving the observed image u_0,

$$\tfrac{1}{2} \int_\Omega (u - u_0)^2 \, dx = \sigma^2. \tag{10}$$

This constraint uses *a priori* information that the standard deviation of the noise is σ (it is also assumed that the noise is normally distributed with mean zero, *i.e.* $\int u \, dx = \int u_0 \, dx$.) In most practical cases this parameter will not be known and the success of the method will require a good estimate of its value. To solve this minimization problem one would usually solve its Euler-Lagrange equation, namely

$$-\nabla \cdot \left(\frac{\nabla u}{\| \nabla u \|} \right) + \lambda (u - u_0) = 0, \qquad \text{in } \Omega, \tag{11}$$

subject to $\partial_{\mathbf{n}} u = 0$ on $\partial\Omega$.

The solution procedure proposed in [89] uses a parabolic equation with time as an evolution (scale) parameter, or equivalently, the gradient descent method. This is

$$\partial_t u - \nabla \cdot \left(\frac{\nabla u}{\| \nabla u \|} \right) + \lambda \left(u - u_0 \right) = 0, \tag{12}$$

in Ω, for $t > 0$, with homogeneous Neumann boundary conditions $\partial_{\mathbf{n}} u = 0$ on $\partial\Omega$ and $u\left(0, x\right) = u_0$ is the observed image used as initial condition. For the parameter λ they suggested a dynamic value $\lambda\left(t\right)$ estimated by Rosen's gradient-projection method, which as $t \to \infty$ converges to

$$\lambda = -\frac{1}{2\sigma^2} \int_{\Omega} \left[\frac{\nabla u^{\mathrm{T}} \left(\nabla u - \nabla u_0 \right)}{\| \nabla u \|} \right] dx. \tag{13}$$

The Rudin-Osher-Fatemi (ROF) model, in its original form, presents several practical challenges [1]. The model has been extensively studied and improved upon by many scientists [1, 109, 100, 11, 40, 65, 95, 101, 107, 76, 19, 59, 23, 90, 75]. Two of the most relevant improvements to the method were proposed by Marquina and Osher [65] and Blomgren, Chan and Mulet [11]. In [65], the authors proposed a different version of the transient parabolic equation that helps speed up the convergence of the time-marching scheme. The new evolution equation is

$$\| \nabla u \| \nabla \cdot \left(\frac{\nabla u}{\| \nabla u \|} \right) + \| \nabla u \| \lambda K * \left(K * u - u_0 \right) = 0, \qquad \text{in } \Omega, \text{ for } t > 0, \tag{14}$$

where $K\left(x\right)$ is a blurring operator (heat kernel). This approach fixes the staircase problem of the original scheme and is used for removal of both blur and noise. In [11], the authors introduced a new approach considering a regularizing functional of the type

$$R\left(u\right) = \int_{\Omega} \| \nabla u \|^p \, dx, \qquad p \in \left[1, 2\right]. \tag{15}$$

For an exponent $p = 1$, one has the TV-norm and when $p = 2$, one would be using the L_2-norm. This approach was studied further in [95] where the following evolution equation was proposed:

$$\partial_t u - \nabla \cdot \left(\| \nabla u \|^{p-2} \nabla u \right) + \lambda (u - u_0) = 0, \qquad \text{in } \Omega, \text{ for } t > 0. \tag{16}$$

Today, the TV-based methods are very well established in the image processing community. They are regarded as the most appropriate and powerful tools for signal reconstruction.

Jonsson, Huang and Chan [48] introduced TV regularization in positron emission tomography (PET) because of its superb noise removal capabilities while capturing sharp edges without oscillations. They modified the standard expectation maximization (EM) for PET to incorporate the TV regularization which resulted in a robust algorithm independent of the amount of regularization. This is equivalent to minimizing

$$\min_u \alpha \int_\Omega \sqrt{|\nabla \Phi|^2 + \beta} d\Omega + \sum_{v=1}^{V} u(v) - \sum_{d=1}^{D} n_d \log Pu(d), \tag{17}$$

where n_d is the photon count (Poisson process) for a detector pair indexed by d, $d = 1, \ldots, D$, $u(v)$, $v = 1, \ldots, V$, denote the intensity within voxel v, P is the detection probability matrix, $n_d = Pu(d)$ is the mean value of counts, $\Phi = \sum_{v=1}^{V} u(v) \varphi_v$ is a linear interpolation[2] of the vector u, β is a small number used to reduce the ill-posedness of the problem, and α is a free parameter chosen by trial and error. The authors argued that their TV regularized EM-algorithm is far better that the standard EM-method when it comes to convergence and enhancement of object edges, better than the standard EM-method at reconstructing large flat regions, and comparable to the standard EM-method for

[2] φ_v is a piece-wise linear function, such that $\varphi_v = 1$ on the center of the voxel v and zero on all other centers

smaller constant intensity regions.

Panin, Zeng and Gullberg [77] proposed a similar approach in the form of an iterative Bayesian reconstruction where the regularization norm is included in the one step late-expectation maximization (OSL-EM) algorithm. They extended the TV norm minimization constraint to the field of single positron emission computed tomography (SPECT) image reconstruction with a Poisson noise model. The authors proposed the following minimization problem (Tikhonov iterative method [105])

$$\min_{u} \left\{ \tfrac{1}{2} \left\| Au - u_0 \right\|^2 + \beta \, \mathrm{TV}\left(u\right) \right\}, \tag{18}$$

where A is a linear operator, $\mathrm{TV}\left(u\right)$ serves as a regularization functional and β is a regularization parameter that controls the weight applied to the minimization of the regularization term relative to the minimization of the residual norm. This TV regularization scheme, when apply to SPECT, provides reconstructed images that have attractive features, such as the identification of distinguishable sharp edges.

Persson, Bone and Elmqvist [84] extended the TV norm formulation from 2-D to 3-D and incorporated it into an ordered subsets EM algorithm for limited view angle acquisition geometry in gamma camera imaging (ectomography). They modified Green's algorithm [42]

$$u_i^{n+1} = \frac{u_i^n}{\sum_j c_{ij} + \beta \left(\partial / \partial u_i\right) \mathrm{TV}\left(u^n\right)} \sum_j \frac{c_{ij} p_j}{\sum_k c_{ij} u_k^n}, \tag{19}$$

where u_i^n is the estimate of the intensity of pixel i after n iterations, c_{ij} is the contribution of image pixel i to projection pixel j, β is a parameter that can be interpreted as the relative strength of the prior compared with the data in

the image estimate[3], p_j is the component j of the projection data set $\mathbf{p}$, and $\mathrm{TV}(u)$ is used as the energy function [58]. The authors called their algorithm TV3D-EM, and evaluated it using a modeled point spread function and digital phantoms. The reconstructed images, when compared with those reconstructed with the 2-D filtered back-projection algorithm, show perceived improvement in quality. The TV3D-EM yielded a reduction in artifacts, caused by the incomplete angular sampling of a limited view angle system, while the noise level was controlled.

Kisilev, Zibulevsky and Zeevi [52] incorporated the wavelet transform (WT) and TV based regularization procedures into the maximum likelihood (ML) framework, embedded into the iterative processes (reconstruction processes) of the EM algorithm and the conjugate barrier (CB) algorithm for PET. Their approaches involve a similar iterative formulation for the penalized EM algorithm (19), and the following two iterative steps for the CB algorithm [9]

$$\begin{array}{ll} \text{step 1}: & u^{k+1} = \nabla u^* \left(\xi^{k+1}\right) \\ \text{step 2}: & \xi^{k+1} = \xi^k - \frac{\gamma^0}{\sqrt{k}} \left\|\nabla L\left(u^k\right)\right\|_\infty \nabla L\left(u^k\right) \\ \text{where} & \nabla L\left(u_v\right) = p\left(v\right) - \sum\limits_{d=1}^{D} \frac{n_d p(v,d)}{\sum\limits_{v'=1}^{V} u_{v'} p(v,d)} + \mu \mathrm{TV}\left(u\right), \end{array} \tag{20}$$

where h^* is the so called conjugate function of h:

$$h^*\left(\xi\right) = \sup_{u\in\Omega} \left[\xi^{\mathrm{T}} u - h\left(u\right)\right], \qquad h\left(u\right) = \begin{cases} \left\|u\right\|_p, & u \in \Omega \\ +\infty, & u \notin \Omega \end{cases}, \tag{21}$$

ξ is called the conjugate image, so that $\xi, \lambda \in \mathbb{R}^V$, γ^k is a positive step size at the k-th iteration, and γ^0 is a small positive constant. The authors concluded that the combination of the CB algorithm with the TV penalty achieves the best

[3] As $\beta \to 0$ the algorithm approaches the ML-EM solution.

contrast to noise trade-off, and that it improves the contrast and suppresses noise simultaneously.

More recently, Zhang and Froment [126] developed a Fourier-based tomographic reconstruction and regularization method from given parallel x-ray projections. They considered a constrained optimization problem of the form

$$\text{find } u^* \in U \quad \text{such that } \mathrm{TV}\left(u^*\right) = \min_{u \in U} \mathrm{TV}\left(u\right), \tag{22}$$

where U is the constraint space of images which satisfy the boundary condition

$$U = \left\{ \begin{array}{l} u \in \mathrm{R}^{N^2} : F_{m,n} \in \left[F^-_{m,n}, F^+_{m,n}\right] \\ \forall m,n = -\frac{N}{2}, \cdots, \frac{N}{2} - 1 \end{array} \right\}, \tag{23}$$

in which $F_{m,n}$ are the Fourier coefficients of the discrete image $u_{m,n}$ of size $N \times N$ on the Cartesian grid. Since TV is a convex function and U is a convex set, any solution u^* of (22) is given by $u^* = P\left(u^* - t \cdot g\left(u^*\right)\right)$, for $t > 0$, where P is the projector onto U that minimizes the distance and $g\left(u\right)$ a subgradient of $\mathrm{TV}\left(u\right)$ at u. The authors' experiments on the well-known Shepp-Logan head phantom [93], show that this approach outperforms the following classical reconstruction methods both in terms of PSNR (an objective mean-square error) and visual quality: direct Fourier method (DFM), filtered back-projection (FBP), and Tikhonov iterative method (TIM).

Sidky, Kao and Pan [94] developed and investigated an iterative image reconstruction algorithm based on the minimization of the image TV norm that applies to both fan-beam and cone-beam computed tomography (CT). This model aims to reconstruct images from sparse or insufficient data problems that may occur due to practical issues of CT scanning (including the few-view, limited-angle, and bad-bin problems.) The TV algorithm that they developed

aims at finding u by implementing the following optimization scheme [16]

$$\min \|u\|_{\mathrm{TV}} \quad \text{such that} \quad \mathbf{M}u = g, \quad u_j \geq 0. \tag{24}$$

In the algorithm, the authors seek to obtain an image represented by the finite vector u from the knowledge of the data vector g and the system matrix $\mathbf{M}$. The minimization of the image TV is carried out by the gradient descent method, and the constraints imposed by the known projection data are incorporated by projection on convex sets (POCS) [7]. They demonstrated and validated the proposed TV algorithm for image reconstruction in various sparse or insufficient data under "ideal" conditions. Also, they presented preliminary results indicating that the TV algorithm seems to be effective on sparse data problems in the presence of signal noise.

Asaki, Campbell, Chartrand, Powell, Vixie and Wohlberg [2] applied TV regularization methods to Abel inversion tomography. The inverse Abel transform tomography is formulated as a functional minimization problem:

$$\min_u F(u) = \min_u \left\{ \|Pu - u_0\|_{\mathrm{d}} + \alpha \mathrm{TV}(u) \right\}, \tag{25}$$

where $\|\cdot\|_{\mathrm{d}}$ is an appropriate data fidelity norm, $\mathrm{TV}(u)$ is the regularization term determined by a probability model of the types of objects we expect, and α is a parameter that should lead to a solution with data fidelity norm equal to the known or estimated variance of the data noise. The authors treated the noise as it if where stationary Gaussian white noise, even though typical experiments are dominated by signal-dependent Poisson noise. Their experimental results showed favorable characteristics of noise suppression and density discontinuity preservation. They also introduced an adaptive TV method that employs a modified discrete gradient operator acting only apart from data-determined

density discontinuities. The authors claim that this method provides improved density level preservation relative to the basic TV method.

3 Preliminary Studies

The image processing techniques we are employing in this work are extensions based on previous work of the main PI. In Blomgren-Chan [12], the ROF TV approach was extended to vector valued images. In the context of [12] the main interpretation was RGB color vectors, but the approach readily extends to other vector, or tensor field images. Further extensions relevant to the current work were explored in [11], and [14]; and a simple, yet extremely effective computational scheme was developed in [13]; the basic idea of feature-driven adaptivity was introduced in [99].

The CI has extensive experience in the electron tomography field; ET of multicomponent biological structures were investigated in [80]; mitochondrial crista junctions examined in [81]; membrane architecture of mitochondria in neurons of the central nervous system studied in [79]; and methods and results of cutting edge ET described in [78, 37, 36].

Parameter-Free Adaptive Total-Variation-Based Noise Removal and Edge Strengthening for Mitochondrial Structure Extraction. In previous work we implemented a variation of Blomgren, Chan and Mulet's [11] version of the fully nonlinear ROF [89] Euler-Lagrange equation as modified by Marquina and Osher [65],

$$\partial_t u - \| \nabla u \| \nabla \cdot \left(L \left(\| \nabla u \|^{p-2} \right) \nabla u \right) + \Lambda \left(u - u_0 \right) = 0, \tag{26}$$

defined in the domain Ω with boundary conditions $\partial_{\mathbf{n}} u = 0$ on $\partial \Omega$ (where $\mathbf{n}$ is the unit normal vector to the boundary of the domain Ω). The Neumann

boundary conditions should guarantee that the filtering does not significantly affect the average gray value of the image. The initial condition is the observed image $u(0,x) = u_0(x)$, in Ω. The model can be regarded as an "adaptive TV model with morphological convection and anisotropic diffusion." Unlike the approach in [89], we implemented a user-independent choice of all the parameters in the model. We start by estimating the unknown noise-level. In this work we assumed that the image has been perturbed by additive Gaussian noise, $u_0 = u + \eta$, hence the variance of the noisy image has to be equal to the sum of the variance of the true image and the variance of the noise, $\sigma^2_{u_0} = \sigma^2_{G_\sigma * u_0} + \sigma^2_\eta$. Here, the variance of the (unknown) true image is approximated by the variance of the convolved noisy image. This parameter will be updated iteratively.

For the parameter λ, we implemented a variation of the method suggested in [89]. Instead of integrating (or summing) over the domain, Ω, we implemented a pixel-wise $\Lambda \equiv \|\nabla u\| \lambda$ as (with a little abuse of notation)

$$\Lambda = -\frac{1}{2\sigma^2}\left[u_x\left(u_x - (u_0)_x\right) + u_y\left(u_y - (u_0)_y\right)\right]. \tag{27}$$

The dynamic parameter Λ has the following attributes:

1. The smaller the value of Λ, the more the diffusion contributed by the forcing term. Analogously, the larger the value of Λ, the lesser the diffusion contributed by the forcing term.

2. At the beginning of the scale-marching iterations the gradients $u_x \approx (u_0)_x$, and $u_y \approx (u_0)_y$, therefore the terms $u_x - (u_0)_x$ and $u_y - (u_0)_y$ are very small and the forcing term tends to contribute more to the diffusion process. In areas where u_x and u_y are large (i.e. near edges), these values compensate for the small values of $u_x - (u_0)_x$ and $u_y - (u_0)_y$.

3. As iterations evolve the terms $u_x - (u_0)_x$ and $u_y - (u_0)_y$ get larger. Near

edges, the forcing term prevents diffusion and helps reach convergence.

We can also get an a posteriori estimate to the variance of the noise σ^2 by integrating (or summing) over the domain after convergence,

$$\sigma^2 = -\tfrac{1}{2}\int_\Omega \frac{1}{\Lambda}\left[u_x\left(u_x - (u_0)_x\right) + u_y\left(u_y - (u_0)_y\right)\right]dx. \tag{28}$$

The diffusion tensor $L\left(\|\nabla u\|^{p-2}\right)$ incorporates the parameter $1 \le p \le 2$, as suggested in [12]. The diffusion tensor becomes

$$L\left(\|\nabla u\|^{p-2}\right) = \begin{bmatrix} \|\nabla u\|^{p_x-2} & -\|\nabla u\|^{p_{xy}-2} \\ -\|\nabla u\|^{p_{xy}-2} & \|\nabla u\|^{p_y-2} \end{bmatrix}, \tag{29}$$

where p_x, p_y, p_{xy}, are the following unnormalized Gaussians $p_x = 1 + e^{-\hat{u}_x^2/4\sigma^2}$, $p_y = 1 + e^{-\hat{u}_y^2/4\sigma^2}$, $p_{xy} = 1 + e^{-\left(\hat{u}_x^2+\hat{u}_y^2\right)/4\sigma^2}$. In these equations, $\hat{u}_x$ and $\hat{u}_y$ are the gradients of the convolved noisy image $G_\sigma * u_0$ used to estimate the unknown parameter σ. The dynamic parameters p_x, p_y, p_{xy}, have the following attributes:

1. For every pixel in the image, the parameters take values: $1 \le p_x \le 2$, $1 \le p_y \le 2$ and $1 \le p_{xy} \le 2$.

2. When $p_x = 1$, $p_y = 1$ or $p_{xy} = 1$ the model uses the TV-norm in the corresponding direction, and when $p_x = 2$, $p_y = 2$ or $p_{xy} = 2$, the model uses the L_2-norm in the corresponding direction.

3. When the parameters $1 < p_x < 2$, $1 < p_y < 2$ and $1 < p_{xy} < 2$, the model interpolates between both norms.

Experimental Results. The mitochondrial images produced by the electron microscope are of extremely low contrast (see Figure 1(a)). If we plot the distribution of intensities of the image we observe that the intensity range is

very narrow. It does not cover the potential range of gray tones [0, 255], and is missing the high and low values that would result in good contrast (see Figure 1(a)). To improve the contrast in the image we spread the intensity values over the full range of the image by a process called histogram equalization. Figure 2(a-b) shows the mitochondrion image after the histogram equalization and its corresponding image histogram. This process notably improves the contrast of the image which becomes better suited for our dynamic noise removal and edge strengthening model.

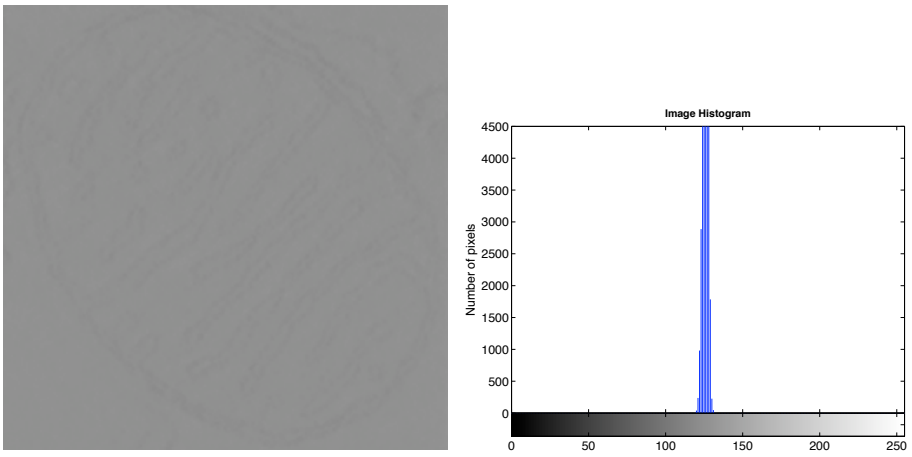

Figure 1: (a-left) Extremely low contrast electron microscope mitochondrion image. (b-right) Image histogram: the intensity range is very narrow.

After the histogram equalization we estimate the value of the variance of the noise as described above, $\sigma_\eta^2 = \sigma_{u_0}^2 - \sigma_{G*u_0}^2$. This value will be dynamically updated until the model reaches convergence using (18). Figure 3 (a-b) illustrates the treated image and its contours. We can observed that the treated image presents better characteristics for either automated or manual segmentation. Figures 4 (a-b) and 5 (a-b) show the final values of the adaptive parameters p_x, p_y, p_{xy} and Λ.

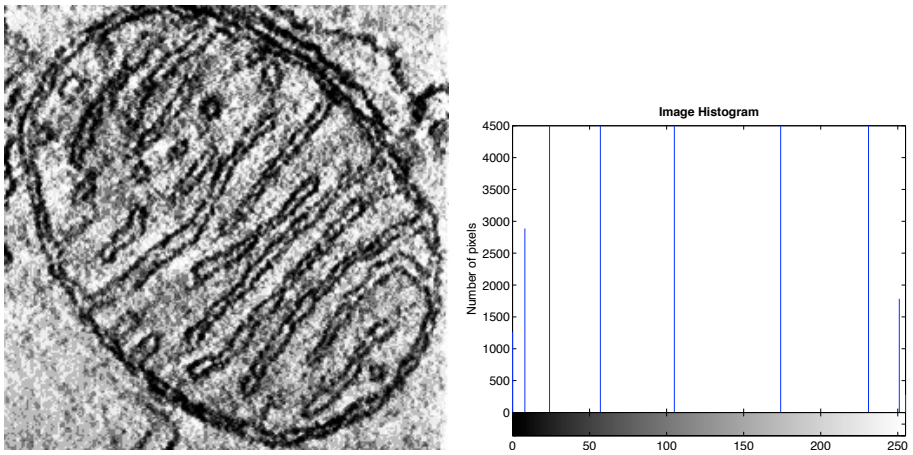

Figure 2: (a-left) Mitochondrion image after histogram equalization. (b-right) Image histogram: the intensity range is spread out over the range [0, 255].

4 Research Design and Methods

The research work comprises the following stages: 1) Estimation of the parameters of the noise incorporated into the ET processes, 2) development of the Total Variation based noise removal and structure enhancement algorithm, 3) Implementation of the numerical solution, and 4) Incorporation of the algorithm into open source ET reconstruction software.

Noise Estimation. In order to develop efficient image processing techniques, it is required that certain types of basic patterns be extracted from the noisy data. Most classical techniques are appropriate in the presence of high (uniform) SNR and Gaussian noise with independent identically distributed (i.i.d.) samples. But, even small deviation from these assumptions can severely deteriorate the performance of the filtering techniques [57]. SNR may also vary significantly from region to region. The presence of unwanted background patterns (structure noise) can degrade the performance of most filters. We will expand the capabilities of the techniques based on analysis of variance (ANOVA)

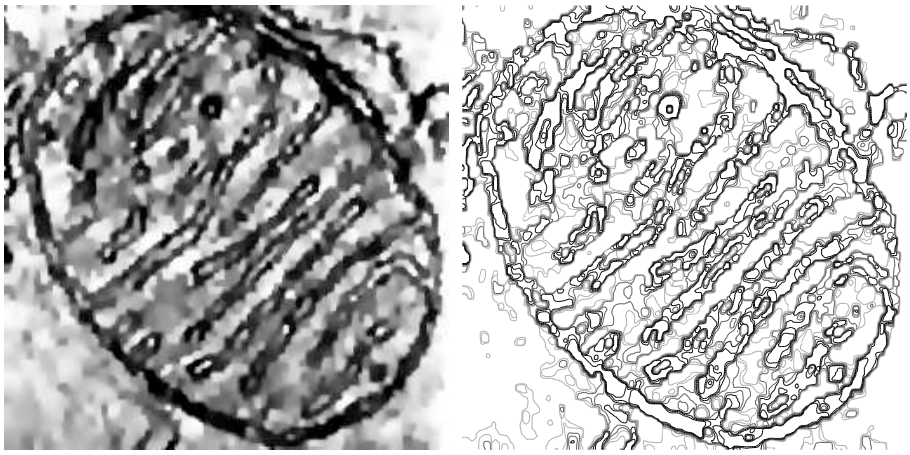

Figure 3: (a-left) Mitochondrion image after being treated with the dynamic model. (b-right) Contours of the image.

to study the noise patterns incorporated into the three-dimensional data generated through ET. It has been argued in [57] that the F-statistics associated with the ANOVA model is optimum for the case of testing against alternatives for Gaussian noise of unknown variance. Furthermore, that it maximizes the probability of detection for all alternatives and among all invariant tests with respect to shifting, scaling, and orthogonal transformation of the data. In the event that the data exhibit non-Gaussian noise, alternative approaches can be used, as the ones involving generalized versions of partition tests [56, 50, 28, 29, 62, 53], or the extensions to the stochastic approximation methodology as suggested in [62, 53]. From a practical point of view we intend to adapt algorithms from available software such as SIMEX [25, 98, 85, 86], to evaluate the noise patterns in three-dimensional ET based on benchmarks, noise-only reconstruction, and equipment manufacturer's calibration procedures.

Total Variation Based Noise Removal Algorithm. We will derive a constrained optimization numerical algorithm for the removal of noise in 3-D electron tomograms. We will use an approach similar to the one in [89] that

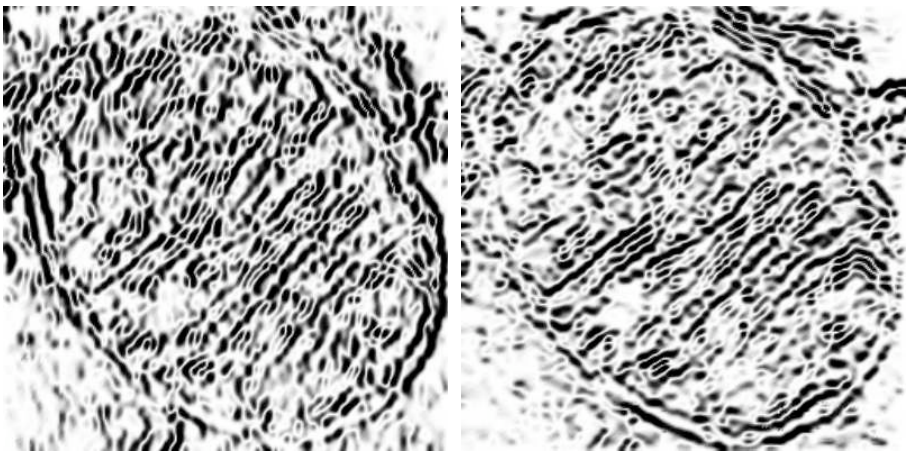

Figure 4: (b-left) Adaptive parameter p_x. (a-right) Adaptive parameter p_y.

minimizes the total variation of the data subject to constraints involving the statistics of the noise. This is a mature and very well established methodology in the computer vision community. It has been extensively studied and improved upon and it is considered the most appropriate for the subject of image restoration. It was designed with the explicit goal of preserving sharp discontinuities (edges) in images while removing noise and other unwanted fine scale detail [22]. This will allow the enhancement of the mitochondrial structure in the very same process when the noise is being removed. Our constrained minimization problem will be:

$$\min_u \int_\Omega |\nabla u|. \tag{30}$$

Here, $\Omega \in \mathbb{R}^3$ represents the image domain, which in our case is the 3-D tomogram. The constraints of the optimization will force the minimization to take place over images that are consistent with our knowledge about the noise statistics. We will arrive to an Euler-Lagrange equation of the type

$$\nabla \cdot \left(G_1 \left(\|\nabla u\| \right) \nabla u \right) - G_2 \left(\|\nabla u\| \right) (u - u_0) = 0, \tag{31}$$

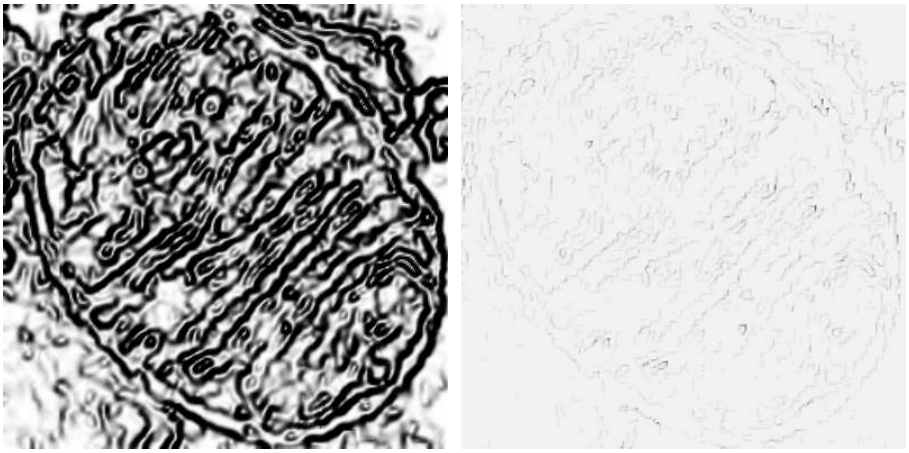

Figure 5: (a-left) Adaptive parameter p_{xy}. (b-right) Adaptive parameter Λ.

in Ω, with $\partial u/\partial \mathbf{n} = 0$ on the boundary $\partial\Omega$. To solve this problem, we will employ a parabolic equation with time as a scale (evolution) parameter. This is

$$\partial_t u - \nabla \cdot \left(G_1 \left(\|\nabla u\| \right) \nabla u \right) + G_2 \left(\|\nabla u\| \right) \left(u - u_0 \right) = 0, \tag{32}$$

for $t > 0$, in Ω, with $\partial u/\partial \mathbf{n} = 0$ on the boundary $\partial\Omega$, and the 3-D tomogram $u\left(0, x, y, z\right) = u_0\left(x, y, z\right)$ as initial condition.

The main difference between our proposed model and the ones firmly established in the computer vision community lies in the terms $G_1\left(\|\nabla u\|\right)$, and $G_2\left(\|\nabla u\|\right)$. These terms will be specifically tailored to the removal of noise and structural enhancement of 3-D mitochondria tomograms. The study of the noise incorporated into 3-D ET will allow the design of these two terms. $G_1\left(\|\nabla u\|\right)$, will be designed as a diffusion tensor that steers the diffusion process in such a way that the eigenvectors prescribe the diffusion directions and the corresponding eigenvalues determine the amount of diffusion along these directions. $G_2\left(\|\nabla u\|\right)$ will be designed in such way that the bias term (forcing term) will spare the user from choosing an stopping time. Both terms will also include

dynamic parameters based on local information and noise patterns. This will allow image reconstruction with minimum human intervention.

Implementation of the Numerical Solution. Digital images are given on discrete (regular) grids. This lends itself for discretizing the PDEs to obtain numerical schemes that can be solved on a computer. Because of their favorable stability and efficiency properties, semi-implicit schemes have been the methods of choice for the scale discretization [17, 49, 4, 5, 116, 113, 68, 55, 87, 69, 43, 45, 44, 26]. As for the space discretization, the most popular choices are finite difference [17, 116, 113] and finite element methods [49, 5, 4, 26, 87, 116, 113] (in that order of preference). We chose to discretize the space using finite difference because of its simplicity and straight forward implementation. The starting point for the numerical implementation is to partition the geometry (domain) into small units (voxels) of simple shape (cube). This will constitute our numerical space (grid). Once we have our grid, the idea is to approximate the partial derivatives by differences in the three directions. In this case, we need to perform discretizations in scale and space. We perform the semi-discretization in scale by letting $N \in \mathbb{N}$, and $k = T/N$ be fixed numbers[4], and letting $u(0, x, y, z) = u_0(x, y, z)$ in Ω. Then, we can look for a function u_n for every $n = 1, \ldots, N$, such that it is a solution to the equation

$$\frac{u_n - u_{n-1}}{k} - \nabla \cdot \left(G_1 \left(\|\nabla u_{n-1}\| \right) \nabla u_n \right) + G_2 \left(\|\nabla u_{n-1}\| \right) (u_{n-1} - u_0) = 0. \quad (33)$$

It is shown in [49, 5] that there exist unique variational solutions u_n of the expression above at every discrete scale step, for which the following stability

[4]Here, T represents the last scale state we want to reach.

estimates hold:

$$\| u_n \|_2 \leq \| u_0 \|_2 , \qquad \| u_n \|_\infty \leq \| u_0 \|_\infty , \qquad \text{for} n = 1, \ldots, N \quad \text{on } \Omega$$

$$\sum_{n=1}^{N} \| \nabla u_n \|_2^2 \, h \leq C, \qquad \sum_{n=1}^{N} \| u_n - u_{n-1} \|_2^2 \leq C, \qquad \text{on } \Omega , \tag{34}$$

where C is a general (large) constant[5]. To discretize the problem in space we can write the partial derivatives

$$\begin{aligned} &\tfrac{u_n - u_{n-1}}{k} - \tfrac{\partial}{\partial x} \left(G_1 \left(\| \nabla u_{n-1} \| \right) \partial_x u_n \right) - \tfrac{\partial}{\partial y} \left(G_1 \left(\| \nabla u_{n-1} \| \right) \partial_y u_n \right) + \\ &- \tfrac{\partial}{\partial z} \left(G_1 \left(\| \nabla u_{n-1} \| \right) \partial_z u_n \right) + G_2 \left(\| \nabla u_{n-1} \| \right) (u_{n-1} - u_0) = 0 \end{aligned} \tag{35}$$

$$\begin{aligned} &\tfrac{u_n - u_{n-1}}{k} - \partial_x G_1 \left(\| \nabla u_{n-1} \| \right) \partial_x u_n - G_1 \left(\| \nabla u_{n-1} \| \right) \partial_{xx} u_n + \\ &- \partial_y G_1 \left(\| \nabla u_{n-1} \| \right) \partial_y u_n - G_1 \left(\| \nabla u_{n-1} \| \right) \partial_{yy} u_n + \\ &- \partial_z G_1 \left(\| \nabla u_{n-1} \| \right) \partial_z u_n - G_1 \left(\| \nabla u_{n-1} \| \right) \partial_{zz} u_n + \\ &+ G_2 \left(\| \nabla u_{n-1} \| \right) (u_{n-1} - u_0) = 0 \end{aligned} \tag{36}$$

Incorporation of the Algorithm into Open Source Software. All of the algorithms designed for the reduction of noise and enhancement of structures in electron tomography will be made available to the developers of open source electron microscopy software. We plan to contact the developers of the most popular ET reconstruction packages (IMOD, SPIDER, Protomo, SerialEM, EM3D, XMIPP, TOM, EMAN/EMAN2, and UCSF tomography) to share with them the algorithms and pseudo-code produced as deliverables in the proposed work. We will also made the algorithms and pseudo code available online where developers of other ET software packages can download them.

[5]Here, h represents a typical element size.

5 Human Subjects

Not applicable in this section of the 398.

6 Vertebrate Animals

Not applicable in this section of the 398.

7 Select Agent Research

Not applicable in this section of the 398.

8 Resource Sharing

Sharing the results of this project is an important aspect of our proposed activities and will be carried out in several different ways. We would like to make our results available both to the structural biology community and the image processing community. Our plan includes the following:

Presentations at national scientific meetings. We are expecting to produce at least one scientific communication per year. Depending of the topic of the communication, we would like to present our findings in the following scientific meetings: Microscopy & Microanalysis, IEEE International Symposium on Biomedical Imaging, and IEEE International Conference on Image Processing. It is expected that the investigators from our team will be active participants of the discussions at these meetings.

Publications in scientific journals. The scientific communications resulted from our research will be submitted for publication to scientific journals in the field. The most likely outlet for these communications are the Journal

of Structural Biology, the Nature Structural & Molecular Biology Journal, and the IEEE Transactions on Image Processing.

Incorporation into open source software. All of the algorithms designed for the reduction of noise and enhancement of structures in electron tomography will be made available to the developers of open source electron microscopy software. We plan to contact the developers of the most popular ET reconstruction packages (IMOD, SPIDER, Protomo, SerialEM, EM3D, XMIPP, TOM, EMAN/EMAN2, and UCSF tomography) to share with them the algorithms and pseudo-code produced as deliverables in the proposed work.

Online publication. The results of the proposed research will be also made available to the public at large via a dedicated website. We plan to set up an email account specially for the purpose of facilitating the communication between people interested in our results and the investigators.

The proposed research project has been submitted for funding in response to the NIH request for applications: "Innovations in Biomedical Computational Science and Technology (R01)", in collaboration with Professors Peter Blomgren and Terry Frey.

References

[1] R. Acar and C.R. Vogel. Analysis of total variation penalty methods for ill-posed problems. *Inverse Problems*, 10(6):1217–1229, 1994.

[2] T.J. Asaki, P.R. Campbell, R. Chartrand, C. Powell, K.R. Vixie, and B.E. Wohlberg. Abel inversion using total variation regularization: Applications. *Inverse Problems in Science and Engineering*, 14(8):873–885, 2006.

[3] C. Bajaj, Z. Yu, and M. Auer. Volumetric feature extraction and visualization of tomographic molecular imaging. *Journal of Structural Biology*, 144(1/2):132–143, 2003.

[4] E. Bänsch and K. Mikula. A coarsening finite element strategy in image selective smoothing. *Computing and Visualization in Science*, 1(1):53–61, 1997.

[5] E. Bänsch and K. Mikula. Adaptivity in 3D image processing. *Computing and Visualization in Science*, 4(1):21–30, 2001.

[6] G.I. Barenblatt, M. Bertsch, R. Dal Passo, and M. Ughi. A degenerate pseudo-parabolic regularization of a nonlinear forward-backward heat equation arising in the theory of heat and mass exchange in stably stratified turbulent shear flow. *SIAM Journal on Mathematical Analysis*, 24(6):1414–1439, 1993.

[7] H.H. Barret and K.J. Myers. *Foundations of Image Science*, chapter 15. John Wiley & Sons, Inc., Hoboken, 2004.

[8] W.T. Baxter, A. Leith, and J. Frank. SPIRE: The SPIDER reconstruction engine. *Journal of Structural Biology*, 157(1):56–63, 2007.

[9] A. Ben-Tal and A. Nemirovski. The conjugate barrier method for non-smooth convex optimization. Technical Report 5/99, Minerva Optimizaion Center Technion, Technion City, 1999.

[10] B. Benhamouda. Parameter adaptation for nonlinear diffusion in image processing. Master's thesis, University of Kaiserslautern, Kaiserslautern, 1994.

[11] P. Blomgren, T. Chan, and P. Mulet. Extensions to total variation denoising. In *Proceedings of Society of Photo-Optical Instrumentation Engineers*, volume 3162, 1997.

[12] P. Blomgren and T.F. Chan. Color TV: Total variation methods for restoration of vector-valued images. *IEEE Transactions on Image Processing*, 7(3):304–309, 1998.

[13] P. Blomgren and T.F. Chan. Modular solvers for constrained image restoration problems using the discrepancy principle. *Numerical Linear Algebra with Applications*, 9(5):347–358, 2002.

[14] P. Blomgren, T.F. Chan, P. Mulet, L. Vese, and W-L Wan. *Numerical Analysis 1999*, volume 420 of *Research Notes in Mathematics*, chapter Variational PDE Models and Methods for Image Processing, pages 43–67. Chapman & Hall/CRC, Boca Raton, 1999.

[15] T. Boudier, J.P. Lechaire, G. Frebourg, C. Messaoudi, C. Mory, C. Colliex, F. Gaill, and S. Marco. A public software for energy filtering transmission electron tomography (EFTET-J): Application to the study of granular inclusions in bacteria from Riftia pachyptila. *Journal of Structural Biology*, 151(2):151–159, 2005.

[16] E. Candes, J. Romberg, and T. Tao. Stable signal recovery from incomplete and inaccurate measurements. *Communications On Pure and Applied Mathematics*, 59(8):1207–1223, 2006.

[17] F. Catté, P.-L. Lions, J.-M. Morel, and T. Coll. Image selective smoothing and edge detection by nonlinear diffusion. *SIAM Journal of Numerical Analysis*, 29(1):182–193, 1992.

[18] A. Chambolle and P.L. Lions. Image recovery via total variation minimization and related problems. *Journal of Numerical Mathematics*, 76(2):167–188, 1997.

[19] T. Chan and S. Esedoglu. Aspects of total variation regularized L^1 function approximation. Technical Report CAM 05-01, University of California Los Angeles, Los Angeles, 2004.

[20] T. Chan, S. Kang, and J. Shen. Total variation denoising and enhancement of color images based on the CB and HSV color models. *Journal of Visual Communication and Image Representation*, 12(4):422–435, 2001.

[21] T. Chan and J. Shen. Mathematical models for local nontexture inpaintings. *SIAM Journal on Applied Mathematics*, 62(3):1019–1043, 2002.

[22] T. Chan and J. Shen. *Image Processing and Analysis: Variational, PDE, Wavelet and Stochastic Methods*. SIAM, Philadelphia, 2005.

[23] Y. Chen, S. Levine, and M. Rao. Variable exponent, linear growth functions in image restoration. submitted to SIAM Journal on Applied Mathematics, 2005.

[24] T. Coleman, Y. Li, and A. Mariano. Segmentation of pulmonary nodule images using total variation minimization. Technical Report TR98-1704, Cornell University, Ithaca, 1998.

[25] J.R. Cook and L.A. Stefanski. Simulation-extrapolation estimation in parametric measurement error models. *Journal of The American Statistical Association*, 89(428):1314–1328, 1994.

[26] U. Diewald, T. Preusser, M. Rumpf, and R. Strzodka. Diffusion models and their accelerated solution in image and surface processing. *Acta Mathematica Universitatis Comenianae*, 70(1):15–34, 2001.

[27] D.C. Dobson and F. Santosa. Recovery of blocky images from noisy and blurred data. *Journal on Applied Mathematics*, 56(4):1181–1198, 1996.

[28] R. Dwyer and L. Kurz. Sequential partition detectors with dependent sampling. *Journal of Cybernetics*, 10:211–232, 1980.

[29] R. Dwyer and L. Kurz. Characterizing partition detectors with stationary and quasi-stationary markov dependent data. *IEEE Transactions on Information Theory*, 32(4):471–482, 1986.

[30] J.J. Fernández and S. Li. An improved algorithm for anisotropic nonlinear diffusion for denoising cryo-tomograms. *Journal of Structural Biology*, 144(1/2):152–161, 2003.

[31] J.J. Fernández and S. Li. Anisotropic nonlinear filtering of cellular structures in cryo-electron tomography. *Computing in Science and Engineering*, 7(5):54–61, 2005.

[32] A.S. Frangakis and F. Forster. Computational exploration of structural information from cryo-electron tomograms. *Current Opinion in Structural Biology*, 14(3):325–331, 2004.

[33] A.S. Frangakis and R. Hegerl. Noise reduction in electron tomographic reconstruction using nonlinear anisotropic diffusion. *Journal of Structural Biology*, 135(3):239–250, 2001.

[34] A.S. Frangakis, A. Stoschek, and R. Hegerl. Wavelet transform filtering and nonlinear anisotropic diffusion assessed for signal reconstruction performance on multidimensional biomedical data. *IEEE Transactions on Biomedical Engineering*, 48(2):213–222, 2001.

[35] J. Frank, M. Radermacher, P. Penczek, J. Zhu, Y. Li, M. Ladjadj, and A. Leith. SPIDER and WEB: Processing and visualization of images in 3D electron microscopy and related fields. *Journal of Structural Biology*, 116(1):190–199, 1996.

[36] T.G. Frey, G.A. Perkins, and M.H. Ellisman. Electron tomography of membrane-bound cellular organelles. *The Annual Review of Biophysics and Biomolecular Structure*, 35:199–224, 2006.

[37] T.G. Frey, C.W. Renken, and G.A. Perkins. Insight into mitochondrial structure and function from electron tomography. *Biochimica et Biophysica Acta*, 1555(1/3):196–203, 2002.

[38] J. Fröhlich and J. Weickert. Image processing using a wavelet algorithm for nonlinear diffusion. Report 104, Laboratory of Technomathematics, University of Kaiserslautern, Kaiserslautern, 1994.

[39] T.D. Goddard, C.C. Huang, and T.E. Ferrin. Visualizing density maps with UCSF Chimera. *Journal of Structural Biology*, 157(1):281–287, 2007.

[40] G. Golub and Mulet P. Chan, T. A nonlinear primal-dual method for total variation-based image restoration. *SIAM Journal on Scientific Computing*, 20(6):1964–1977, 1999.

[41] D.R. Green and J.C. Reed. Mitochondria and apoptosis. *Science*, 281(5381):1309–1312, 1998.

[42] P.J. Green. Bayesian reconstructions from emission tomography data using a modifed EM algorithm. *IEEE Transactions on Medical Imaging*, 9(1):84–93, 1990.

[43] A. Handlovičová, K. Mikula, and A. Sarti. Numerical solution of parabolic equations related to level set formulation of mean curvature flow. *Computing and visualization in Science*, 1(2):179–182, 1999.

[44] A. Handlovičová, K. Mikula, and F. Sgallari. Variational numerical methods for solving nonlinear diffusion equations arising in image processing. *Journal for Visual Communication and Image Representation*, 13(1/2):217–237, 2002.

[45] A. Handlovičová, K. Mikula, and F. Sgallari. Semi-implicit complementary volume scheme for solving level set like equations in image processing and curve evolution. *Numerische Mathematik*, 93(4):675–669, 2003.

[46] M.L. Harlow, D. Ress, A. Stoschek, R.M. Marshall, and U.J. McMahan. The architecture of active zone material at the frog's neuromuscular junction. *Nature*, 409(6819):479–484, 2001.

[47] K. Höllig and J.A. Nohel. A diffusion equation with a non-monotone constitutive function. In J.M. Ball, editor, *Proceedings of NATO/London Mathematical Society Conference on Systems of Partial Differential Equation*, 1983.

[48] E. Jonsson, S.C. Huang, and T. Chan. Total variation regularization in positron emission tomography. Technical Report, University of California Los Angeles, Los Angeles, 1998.

[49] J. Kačur and K. Mikula. Solution of nonlinear diffusion appearing in image smoothing and edge detection. *Applied Numerical Mathematics*, 17(1):47–59, 1995.

[50] P. Kersten and L. Kurz. Bivariate m-interval classifiers with application to edge detection. *Information and Control*, 34(2):152–169, 1977.

[51] S. Kichenassamy. The perona-malik paradox. *SIAM Journal of Applied Mathematics*, 57(5):1328–1342, 1997.

[52] P. Kisilev, M. Zibulevsky, and Y.Y. Zeevi. Wavelet representation and total variation regularization in emission tomography. In *Proceedings of International Conference on Image Processing*, volume 1, pages 702–705, 2001.

[53] J.M. Kowalski. *A Contribution to Robust Detection and Estimation in Dependent Noise*. PhD thesis, Polytechnic University, New York, 1992.

[54] J.R. Kremer, D.N. Mastronarde, and J.R. McIntosh. Computer visualization of three-dimensional image data using IMOD. *Journal of Structural Biology*, 116(1):71–76, 1996.

[55] Z. Krivá and K. Mikula. An adaptive finite volume scheme for solving nonlinear diffusion in image processing. *Journal for Visual Communication and Image Representation*, 13(1/2):22–35, 2002.

[56] L. Kurz. *Nonparametric Methods in Communications*, chapter Nonparametric Detectors Based on Partition Tests. Marcel Dekker, New York, 1977.

[57] L. Kurz and M.H. Benteftifa. *Analysis of Variance in Statistical Image Processing*. Cambridge University Press, Cambridge, 1997.

[58] K. Lange. Convergence of EM image reconstruction with gibbs smoothing. *IEEE Transactions on Medical Imaging*, 9(4):439–446, 1990.

[59] S. Levine, Y. Chen, and J. Stanich. Image restoration via nonstandard diffusion. Technical Report 04-01, Department of Mathematics and Computer Science, Duquesne University, Pittsburgh, 2004.

[60] X. Li and T. Chen. Nonlinear diffusion with multiple edginess thresholds. *Pattern Recognition*, 27(8):1029–1037, 1994.

[61] Y. Li, A. Leith, and J. Frank. Tinkerbell: A tool for interactive segmentation of 3D data. *Journal of Structural Biology*, 120(3):266–275, 1997.

[62] G. Lomp. *Nonlinear Robust Detection and Estimation in Dependent Noise*. PhD thesis, Polytechnic University, New York, 1987.

[63] S.J. Ludtke, P.R. Baldwin, and W. Chiu. EMAN: Semiautomated software for high-resolution single-particle reconstructions. *Journal of Structural Biology*, 128(1):82–97, 1999.

[64] S.P. Mallick, B. Carragher, C.S. Potter, and D.J. Kriegman. ACE: Automated CTF estimation. *Ultramicroscopy*, 104(1):8–29, 2005.

[65] A. Marquina and S. Osher. Explicit algorithms for a new time dependent model based on level set motion for a nonlinear debluring and noise removal. *SIAM Journal on Scientific Computing*, 22(2):387–405, 2000.

[66] D.N. Mastronarde. Dual-axis tomography: An approach with alignment methods that preserve resolution. *Journal of Structural Biology*, 120(3):343–352, 1997.

[67] D.N. Mastronarde. Automated electron microscope tomography using robust prediction of specimen movements. *Journal of Structural Biology*, 152(1):36–51, 2005.

[68] K. Mikula and N. Ramarosy. Semi-implicit finite volume schemes for solving nonlinear diffusion equations in image processing. *Numerische Mathematik*, 89(3):561–590, 2001.

[69] K. Mikula, A. Sarti, and C. Lamberti. Geometrical diffusion in 3-d-echocardiography. In J. Kačur and K. Mikula, editors, *Proceedings of ALGORITMY '97, Conference on Scientific Computing*, volume 67, pages 167–181. Acta Mathematica Universitatis Comenianae, 1998.

[70] J.A. Mindell and N. Grigorieff. Accurate determination of local defocus and specimen tilt in electron microscopy. *Journal of Structural Biology*, 142(3):334–347, 2003.

[71] P. Mrázek and M. Navara. Selection of optimal stopping time for nonlinear diffusion filtering. *International Journal of Computer Vision*, 52(2/3):189–203, 2003.

[72] S. Nickell, F. Forster, A. Linaroudis, W.D. Net, F. Beck, R. Hegerl, W. Baumeister, and J.M. Plitzko. TOM software toolbox: Acquisition and analysis for electron tomography. *Journal of Structural Biology*, 149(3):227–234, 2005.

[73] M. Nitzberg and T. Shiota. Nonlinear image filtering with edge and corner enhancement. *IEEE Transactions on Pattern Analysis and Machine Intelligence*, 14(8):826–833, 1992.

[74] L.G. Ofverstedt, K. Zhang, L.A. Isaksson, G. Bricogne, and U. Skoglund. Automated correlation and averaging of three-dimensional reconstructions obtained by electron tomography. *Journal of Structural Biology*, 120(3):329–342, 1997.

[75] S. Osher, M. Burger, D. Goldfarb, J. Xu, and W. Yin. An iterative regularization method for total variation-based image restoration. *SIAM Multiscale Modeling and Simulation*, 4(2):460–489, 2005.

[76] S. Osher, A. Sole, and L. Vese. Image decomposition and restoration using total variation minimization and the H^{-1} norm. *SIAM Journal on Multiscale Modeling and Simulation*, 1(3):349–370, 2003.

[77] V.Y. Panin, G.L. Zeng, and G.T. Gullberg. Total variation regulated EM algorithm. *IEEE Transactions on Nuclear Science*, 46(6):2022–2210, 1999.

[78] G.A. Perkins and T.G. Frey. Recent structural insight into mitochondria gained by microscopy. *Micron*, 31(1):97–111, 2000.

[79] G.A. Perkins, C.W. Renken, T.G. Frey, and M.H. Ellisman. Membrane architecture of mitochondria in neurons of the central nervous system. *Journal of Neuroscience Research*, 66:857–865, 2001.

[80] G.A. Perkins, C.W. Renken, J.Y. Song, T.G. Frey, S.J. Young, S. Lamont, M.E. Martone, S. Lindsey, and M.H. Ellisman. Electron tomography of large, multicomponent biological structures. *Journal of Structural Biology*, 120(3):219–227, 1997.

[81] G.A. Perkins, J.Y. Song, L. Tarsa, T.J. Deerinck, M.H. Ellisman, and T.G. Frey. Electron tomography of mitochondria from brown adipocytes reveals crista junctions. *Journal of Bioenergetics and Biomembranes*, 30(5):431–442, 1998.

[82] P. Perona and J. Malik. Scale space and edge detection using anisotropic diffusion. *IEEE Transactions on Pattern Analysis and Machine Intelligence*, 12(7):629–639, 1990.

[83] P. Perona, T. Shiota, and J. Malik. Anisotropic diffusion. In B.M. ter Haar Romeny, editor, *Geometry-Driven Diffusion in Computer Vision*, volume 1 of *Computational Imaging and Vision*, pages 72–92. Springer, Kluwer, 1994.

[84] M. Persson, D. Bone, and H. Elmqvist. Total variation norm for three-dimensional iterative reconstruction in limited view angle tomography. *Physics in Medicine and Biology*, 46(3):853–866, 2001.

[85] J. Polzehl and S. Zwanzig. On a symmetrized extrapolation estimator in linear errors-in-variables models. *Computational Statistics & Data Analysis*, 47(4):675–688, 2004.

[86] J. Polzehl and S. Zwanzig. SIMEX and TLS: An equivalence result. WIAS Preprint No. 999, 2004.

[87] T. Preusser and M. Rumpf. An adaptive finite element method for large scale image processing. In *Proceedings of Scale-Space '99*, pages 223–234, 1999.

[88] D.B. Ress, M.L. Harlow, R.M. Marshall, and U.J. McMahan. Methods for generating high-resolution structural models from electron microscope tomography data. *Structure*, 12(10):1763–1774, 2004.

[89] L. Rudin, S. Osher, and Fatemi E. Nonlinear total variation based noise removal algorithm. *Physica D*, 60(1/4):259–268, 1992.

[90] P. Schults, E. Bollt, R. Chartrand, Esedoglu, and K. Vixie. Graduated adaptive image denoising: Local compromise between total variation and isotropic diffusion. Preprint, 2005.

[91] J. Shen. On the foundations of vision modeling I. weber's law and weberized TV restoration. *Physica D*, 175(3):241–251, 2003.

[92] J. Shen. Bayesian video dejittering by BV image model. *SIAM Journal on Applied Mathematics*, 64(5):1691–1708, 2004.

[93] L.A. Shepp and B.F. Logan. The Fourier reconstruction of a head section. *IEEE Transactions on Nuclear Science*, 21:21–43, 1974.

[94] E.Y. Sidky, C.M. Kao, and X. Pan. Accurate image reconstruction from few-views and limited-angle data in divergent-beam CT. *Journal of X-Ray Science and Technology*, 14(2):119–139, 2006.

[95] B. Song. *Topics in Variational PDE Image Segmentation, Inpainting and Denoising*. PhD thesis, University of California Los Angeles, Los Angeles, 2003.

[96] C.O. Sorzano, R. Marabini, J. Velazquez-Muriel, J.R. Bilbao-Castro, S.H. Scheres, J.M. Carazo, and A. Pascual-Montano. XMIPP: A new generation of an open-source image processing package for electron microscopy. *Journal of Structural Biology*, 148(2):194–204, 2004.

[97] D. Sousa and N. Grigorieff. Ab initio resolution measurement for single particle structures. *Journal of Structural Biology*, 157(1):201–210, 2007.

[98] L.A. Stefanski and J.R. Cook. Simulation-extrapolation: The measurement error jackknife. *Journal of The American Statistical Association*, 90(432):1247–1256, 1995.

[99] D. Strong, P. Blomgren, and T.F. Chan. Spatially adaptive local feature-driven total variation image restoration. In *Proceedings of The International Society for Optical Engineering*, volume 3167, pages 222–233, 1997.

[100] D. Strong and T. Chan. Spatially and scale adaptive total variation based regularization and anisotropic diffusion in image processing. Technical Report 46, University of California Los Angeles, Los Angeles, 1996.

[101] D. Strong and T. Chan. Edge-preserving and scale-dependent properties of total variation regularization. *Inverse Problems*, 19(6):165–187, 2003.

[102] C. Suloway, J. Pulokas, D. Fellmann, A. Cheng, F. Guerra, J. Quispe, S. Stagg, C.S. Potter, and B. Carragher. Automated molecular microscopy: The new Leginon system. *Journal of Structural Biology*, 151(1):41–60, 2005.

[103] G. Tang, L. Peng, P.R. Baldwin, D.S. Mann, W. Jiang, I. Rees, and S.J. Ludtke. EMAN2: An extensible image processing suite for electron microscopy. *Journal of Structural Biology*, 157(1):38–46, 2007.

[104] K.A. Taylor, J. Tang, Y. Cheng, and H. Winkler. The use of electron tomography for structural analysis of disordered protein arrays. *Journal of Structural Biology*, 120(3):372–386, 1997.

[105] A.N. Tikhonov. Solution of incorrectly formulated problems and the regularization method. *Soviet Mathematical Doklady*, 4:1035–1038, 1963.

[106] M. van Heel and G. Harauz. Resolution criteria for three dimensional reconstruction. *Optik*, 73:119–122, 1986.

[107] L. Vese and S. Osher. Modeling textures with total variation minimization and oscillating patterns in image processing. *Journal of Scientific Computing*, 19(1/3):553–572, 2003.

[108] L. Vese and S. Osher. Image denoising and decomposition with total variation minimization and oscillatory functions. *Journal of Mathematical Imaging and Vision*, 20(1/2):7–18, 2004.

[109] C.R. Vogel and M.E. Oman. Iterative methods for total variation denoising. *SIAM Journal on Scientific Computing*, 17(1):227–238, 1996.

[110] N. Volkmann. A novel three-dimensional variant of the watershed transform for segmentation of electron density maps. *Journal of Structural Biology*, 138(1/2):123–129, 2002.

[111] J. Weickert. Theoretical foundations of anisotropic diffusion in image processing. In *Proceedings of the 7th TFCV on Theoretical Foundations of Computer Vision*, volume 11 of *Computing Supplement*, pages 221–236, London, 1994. Springer-Verlag.

[112] J. Weickert. *Anisotropic Diffusion in Image Processing.* ECMI Series. Teubner-Verlag, Stuttgart, 1998.

[113] J. Weickert. Coherence-enhancing diffusion filtering. *International Journal of Computer Vision*, 31(2/3):111–127, 1999.

[114] J. Weickert. Coherence-enhancing diffusion of colour images. *Image and Vision Computing*, 17(3):201–212, 1999.

[115] J. Weickert. Efficient image segmentation using partial differential equations and morphology. *Pattern Recognition*, 34(9):1813–1824, 2001.

[116] J. Weickert, B.M.t.H. Romeny, and M.A. Viergever. Efficient and reliable schemes for nonlinear diffusion filtering. *IEEE Transactions on Image Processing*, 7(3):398–410, 1998.

[117] J. Weickert and H. Scharr. A scheme for coherence-enhancing diffusion filtering with optimized rotation invariance. *Journal of Visual Communication and Image Representation*, 13(1/2):103–118, 2002.

[118] J. Weickert and C. Schnörr. PDE-based preprocessing of medical images. *Kunstliche Intelligenz*, 3:5–10, 2000.

[119] R.T. Whitaker and S.M. Pizer. A multi-scale approach to non-uniform diffusion. *Computer Vision, Graphics, and Image Processing: Image Understanding*, 57(1):99–110, 1993.

[120] H. Winkler. 3D reconstruction and processing of volumetric data in cryo-electron tomography. *Journal of Structural Biology*, 157(1):126–137, 2007.

[121] H. Winkler and K.A. Taylor. Focus gradient correction applied to tilt series image data used in electron tomography. *Journal of Structural Biology*, 143(1):24–32, 2003.

[122] H. Winkler and K.A. Taylor. Accurate marker-free alignment with simultaneous geometry determination and reconstruction of tilt series in electron tomography. *Ultramicroscopy*, 106(3):240–254, 2006.

[123] W. Wriggers, P. Chacón, J. Kovacs, F. Tama, and S. Birmanns. Topology representing neural networks reconcile biomolecular shape, structure, and dynamics. *Neurocomputing*, 56:365–379, 2004.

[124] W. Wriggers, R.A. Milligan, and J.A. McCammon. Situs: A package for docking crystal structures into low-resolution maps from electron microscopy. *Journal of Structural Biology*, 133(2/3):85–195, 1999.

[125] C. Yang, P.A. Penczek, A. Leith, F.J. Asturias, E.G. Ng, R.M. Glaeser, and J. Frank. The parallelization of SPIDER on distributed-memory computers using MPI. *Journal of Structural Biology*, 157(1):240–249, 2007.

[126] X.Q. Zhang and J. Froment. Total variation based fourier reconstruction and regularization for computer tomography. In *Proceedings of Nuclear Science Symposium and Medical Imaging Conference*, volume 4, pages 2332–2336, 2005.

[127] Q.S. Zheng, M.B. Braunfeld, J.W. Sedat, and D.A. Agard. An improved strategy for automated electron microscopic tomography. *Journal of Structural Biology*, 147(2):91–101, 2004.

[128] Q.S. Zheng, B. Keszthelyi, E. Branlund, J.M. Lyle, M.B. Braunfeld, J.W. Sedat, and Agard D.A. UCSF tomography: An integrated software suite for real-time electron microscopic tomographic data collection, alignment, and reconstruction. *Journal of Structural Biology*, 157(1):138–147, 2007.

[129] U. Ziese, A.H. Janssen, J.L. Murk, W.J. Geerts, T. Van der Krift, A.J. Verkleij, and A.J. Koster. Automated high-throughput electron tomography by pre-calibration of image shifts. *Journal of Microscopy*, 205(2):187–200, 2002.